

Article

Operational Algorithms for Separable Qubit X States

Demosthenes Ellinas

School of Electrical and Computer Engineering QLab, Technical University of Crete, 73100 Chania, Crete, Greece; ellinas@ece.tuc.gr

Received: 21 March 2019; Accepted: 27 June 2019; Published: 2 July 2019



Abstract: This work motivates and applies operational methodology to simulation of quantum statistics of separable qubit X states. Three operational algorithms for evaluating separability probability distributions are put forward. Building on previous findings, the volume function characterizing the separability distribution is determined via quantum measurements of multi-qubit observables. Three measuring states, one for each algorithm are generated via (i) a multi-qubit channel map, (ii) a unitary operator generated by a Hamiltonian describing a non-uniform hypergraph configuration of interactions among 12 qubits, and (iii) a quantum walk CP map in an extended state space. Higher order CZ gates are the only tools of the algorithms hence the work associates itself computationally with the Instantaneous Quantum Polynomial-time Circuits (IQP), while wrt possible implementation the work relates to the Lechner-Hauke-Zoller (LHZ) architecture of higher order coupling. Finally some uncertainty aspects of the quantum measurement observables are discussed together with possible extensions to non-qubit separable bipartite systems.

Keywords: separability; X states 2; quantum walk; quantum algorithm; quantum simulation

1. Introduction

The framework and previous work: An extensive literature exist of mainly numerical studies of the quantum entanglement found in the density matrices of bipartite quantum systems, via certain matrix distance measures. The starting kick of this research project is a seminal paper of 1998 by Życzkowski et al. [1], where the “separability probability” is introduced as a measure of how often a randomly chosen quantum bipartite system splits into two classically correlated parts. Promoting the manifold of parameters determining the density matrices of the total and the reduced quantum systems into a statistical event space endowed with a distance measure, the “separability probability” can be cast into a geometric probability given e.g., by the ratio of the corresponding volume of separable marginal systems to the total volume of bipartite system in the manifold of parameters.

In this work employing the Hilbert–Schmidt (HS) measure, bipartite systems of 2×2 dimensionality are investigated analytically. The manifold of parameters characterizing a special class of bipartite systems, the so-called two-qubits X mixed states, is a real 7D manifold. Specifically, the density matrices of the marginal systems A and B , described by their corresponding Bloch vector lengths (ball radii) r_A, r_B and the respective volumes have been investigated analytically and numerically. The a priori marginal *separability probability* function has been determined to be

$$p_{sep}^{(\alpha)}(r) = \frac{V_{HS,sep}^{(\alpha)}(r)}{V_{(HS)}^{(\alpha)}(r)},$$

for cases of general coupled qubits ($\alpha = 2 \times 2$) and of the special type of X density matrix ($\alpha = X$). Remarkably constant values for the a priori probabilities have been conjectured and have been corroborated or proved by numerical work or analytic derivations. Analytic calculations in e.g., [2],

show that in terms of the radial *volume function* $f(r) = (1 - r^2)^3$, the scaled volume functions $V_{HS,sep}^{(\alpha)} \propto f(r)$ and $V_{HS}^{(\alpha)} \propto f(r)$, in the case of X states are explicitly

$$V_{HS,sep}^{(X)}(r) = \frac{4\pi^2}{45}(1 - r^2)^3, \tag{1}$$

$$V_{(HS)}^{(X)}(r) = \frac{2\pi^2}{9}(1 - r^2)^3, \tag{2}$$

so the probability distribution $p_{sep}^{(X)}(r)$ reads

$$p_{sep}^{(X)}(r) = \frac{2}{5}, p_{nosep}^{(X)}(r) = \frac{3}{5}, r \in [0, 1) \text{ and } p_{sep}^{(X)}(1) = 1.$$

This remarkable constant probability within the interval $r \in [0, 1)$ has verified previous numerical and analytic conjectures—see, e.g., [3]. Similarly for the general bipartite systems of 2×2 systems, it is known that $p_{sep}^{(2 \times 2)}(r) = \frac{2}{5}, r \in [0, 1)$. Despite numerous numerical and, to a lesser extent, analytic works in this field over the last years, hardly anything has been done with respect to its operational and quantum simulation aspects of those probability distributions.

Outline of paper’s contribution: This work starts providing a motivation for applying operational methodology to simulation quantum statistics of separable states. It proceeds to puts forward three operational algorithms for evaluating separability probability distributions for X states of qubits. Specifically, it is shown that the volume function which determines the separability distribution can be obtained via quantum measurements of certain respective multi-qubit observables.

There are three measuring states, one for each operational algorithm. These states are generated from the original X states under investigation respectively via (i) a multi-qubit channel map, (ii) a unitary operator generated by a Hamiltonian describing a non-uniform hypergraph [4–7], configuration of interactions among 12 qubits, and (iii) a quantum walk completely positive (CP) map in an extended state space. All three proposed algorithms are based on an 12-qubit lattice system with an underlying interaction scheme described by a hypergraph.

Two important connections of the paper with some related research fields as emphasized. First: The building blocks of the algorithms are higher order controlled-not CZ diagonal gates [8–13]. This fact suggests that the formalism and the computational tasks carried out by the algorithms associate them with the field of the so-called Instantaneous Quantum Polynomial-time Circuits (IQP) [14–21]; Second: wrt possible implementation, the work relates itself to the LHZ quantum computation architecture of higher order coupling [22,23].

Structure of the paper: The present introductory chapter concludes offering a motivation of the attempted operational approach to the separability statistics. Section 2 provides all the needed elements for X states and their quantum mechanical aspects that will allow for building up in the sequel the operational framework. The next three Sections 3–5 provide respectively the necessary background and formulation of the three simulation algorithms for the distribution of separability. Section 6 is a brief one that presents some important aspects regarding the computation methodology and implementation possibilities of the algorithms. Section 7 is a closing discussion on the overall operational methodology and on the prospects of applying paper’s ideas to general Bloch vector components functions. Finally, in three appendices, material is included concerning, (Appendix A), the matrix analysis aspects and the proof of the main proposition; (Appendix B) aspects of uncertainties of the quantum measurements presented in previous chapters, while Appendix C shows the underlying hypergraph structure of volume operator and the associated Hamiltonian. In the opening of each chapter, a brief outline of its content is provided.

Motivation of this work: Let a physical phenomenon conjectured to be described statistically by e.g., a Poisson distribution over natural numbers with a fixed mean value. If a realistic statistical experiment is difficult to be set up, sampled and investigated, one could come up with the idea of building an

hitherto unknown simulator e.g., a laser coherent light beam generator. This concept-device could in some way serve the purpose of a quantum simulator i.e., it could be considered as an experimental and theoretical device for simulating the above phenomenon and corroborate or falsify its initial statistical conjecture. This is so, since it is a standard knowledge that a laser beam is generated from an initial state of thermal light photons with Maxwell–Boltzmann energy distribution and that, beyond the lasing threshold, theory and experiment prove the occurrence of a phase transition from thermal photons to photons with energy following Poissonian statistics [24]. The theoretical requirements of such laser light simulator would include developing a set of landmark operations in open quantum systems such as coupling and de-coupling between quantum system and quantum environment, quantum master equation solutions, in terms of CP maps, of the light density matrix, statistical correlations of the laser light beam, distinct thermodynamic features developed during the lasing transition, etc. The laser quantum simulation could additionally provide checks and simulations of statistical questions of interest, questions concerning required resources for the feasibility of the initial statistical conjecture i.e., questions pertaining to the energy, entropy and work resources of the phenomenon, as well as their transformations. Note that here we should distinguish between resources of the initial physical system and those of the simulating quantum system. It is in fact the latter ones i.e., the resources of quantum simulation that would constitute a novel important aspect to be addressed in the field of quantum simulations.

Based on the analogous situation of the laser quantum simulation, similar general ideas can be specified in the present case of simulating the statistics of separable X states. To this end, this work puts forward some hitherto unknown simulator that employs a lattice of 12 qubits and provides versions of some operational algorithms that derive the conjectured probability distribution of pairs of separable qubits in an X form density matrix.

As detailed below, the algorithms describe both closed Hamiltonian systems and also open system operations. More generally, the operational algorithmic methodology put forward here is in fact grounded in a well developed operational methodology of constructing quantum observables and quantum measurements with desired properties—see, e.g., [25] for a general theory, [26] for related quantum optical problems, and [27,28] for problems formulated in quantum mechanical phase space.

2. X States Operational Framework

Chapter’s outline: The X state density matrix is introduced and its Bloch vector components and relevant polynomials thereof are expressed by expectation values of generalized multi-qubit observables. The volume operator and its components are introduced.

The two-qubit density matrix of the so-called “X state” is a special case of bipartite state and reads [29–31],

$$\rho_X = \begin{pmatrix} \rho_{11} & & & \rho_{14} \\ & \rho_{22} & \rho_{23} & \\ & \rho_{32} & \rho_{33} & \\ \rho_{41} & & & \rho_{44} \end{pmatrix}.$$

More specifically, on the basis of 16 elements formed by all possible tensor products of Pauli and unit matrix between themselves,

$$\{\mathbb{I} \otimes \mathbb{I}, X \otimes \mathbb{I}, Y \otimes \mathbb{I}, Z \otimes \mathbb{I}, \mathbb{I} \otimes X, \mathbb{I} \otimes Y, \mathbb{I} \otimes Z, X \otimes X, Y \otimes Y, Z \otimes Z, X \otimes Y, \dots, Y \otimes Z\}.$$

The X-density reads

$$\begin{aligned} \rho_X = & \frac{1}{4}(\mathbb{I} \otimes \mathbb{I} + a_z Z \otimes \mathbb{I} + b_z \mathbb{I} \otimes Z + c_{xx} X \otimes X + c_{xy} X \otimes Y \\ & + c_{yx} Y \otimes X + c_{yy} Y \otimes Y + c_{zz} Z \otimes Z). \end{aligned}$$

The expansion coefficients are linearly related to the original ρ_{ij} matrix elements and, in order to determine them forming the density matrix, we introduce the inner product for 2×2 matrices as $\langle A, B \rangle \equiv \text{Tr}(AB^\dagger)$. Verify that $\langle \mathbb{I} \otimes \mathbb{I}, \rho_X \rangle = \text{Tr}(\mathbb{I} \otimes \mathbb{I} \rho_X) = 1$ and compute the a_z coefficient as $\langle Z \otimes \mathbb{I}, \rho_X \rangle = \text{Tr}(Z \otimes \mathbb{I} \rho_X) = a_z = \rho_{11} + \rho_{22} - \rho_{33} - \rho_{44} \equiv r$, and similarly for the rest of the coefficients.

With the polynomial volume function $f(r)$ of a previous chapter in mind and in order to be able to express powers of variable r as inner products of density matrix with various products of Pauli matrices, we proceed to embed those matrices into an n -fold tensor product of Pauli algebra as follows. Using the generic notation $S_a, a = 1, 2, 3$ for all Pauli matrices, respectively $X \equiv \sigma_x, Y \equiv \sigma_y, Z \equiv \sigma_z$, we introduce their embedding as a map from $\mathbb{C}^{2 \times 2} \ni S_a$ into the n -fold matrix product space $(\mathbb{C}^{2 \times 2})^{\otimes n} \ni S_a^i$, by means of the correspondence $S_a \rightarrow S_a^i$, where

$$S_a^i \equiv S_a^{\otimes(i-1)} \otimes S_a \otimes S_a^{\otimes(n-i)},$$

for $i = 1, 2, \dots, n$.

Next, recall the identity $\text{Tr}A\text{Tr}B = \text{Tr}(A \otimes B)$, which further implies that

$$\langle A, \rho \rangle \langle B, \rho \rangle = \langle A \otimes B, \rho \otimes \rho \rangle,$$

and more generally

$$\langle A_1, \rho \rangle \cdots \langle A_n, \rho \rangle = \langle A_1 \otimes \cdots \otimes A_n, \rho^{\otimes n} \rangle.$$

Then, referring to Equations (1) and (2), and applying the previous identities, we compute that, for the density matrix ρ_X , the following identities are valid (for notational simplicity, the X index is omitted hereafter),

$$1 - r^2 = \langle \mathbb{I}^{\otimes 4} - Z \otimes \mathbb{I} \otimes Z \otimes \mathbb{I}, \rho \otimes \rho \rangle,$$

and

$$(1 - r^2)^3 = \langle \mathbb{I}^{\otimes 12} - 3\mathbb{I}^{\otimes 8} \otimes Z \otimes \mathbb{I} \otimes Z \otimes \mathbb{I} + 3\mathbb{I}^{\otimes 4} \otimes Z \otimes \mathbb{I} \otimes Z \otimes \mathbb{I}, \rho^{\otimes 6} \rangle.$$

Next, define the unitary volume operator $\hat{V} : (\mathbb{C}^{4 \times 4})^{\otimes 6} \rightarrow (\mathbb{C}^{4 \times 4})^{\otimes 6}$ acting on the Hilbert space of six bipartite X states $(\mathbb{C}^{4 \times 4})^{\otimes 6}$ and reads explicitly,

$$\hat{V} \equiv \mathbb{I}^{\otimes 12} - 3\mathbb{I}^{\otimes 8} \otimes Z \otimes \mathbb{I} \otimes Z \otimes \mathbb{I} + 3\mathbb{I}^{\otimes 4} \otimes Z \otimes \mathbb{I} \otimes Z \otimes \mathbb{I}.$$

Recall the volume functions issued in Equations (1) and (2) to compute that

$$V_{HS}^{(X)}(r) = \frac{\pi^2}{2304} \langle \hat{V}, \rho^{\otimes 6}(r) \rangle. \tag{3}$$

Furthermore, by simplifying $A \otimes B$ to AB , the volume operator reads

$$\hat{V} = \mathbb{I}^{\otimes 12} - 3Z^9 Z^{11} + 3Z^5 Z^7 Z^9 Z^{11} - Z^1 Z^3 Z^5 Z^7 Z^9 Z^{11}. \tag{4}$$

Proceeding next by defining variables $a = \mathbb{I}^{\otimes 4}$ and $b = Z \otimes \mathbb{I} \otimes Z \otimes \mathbb{I} \equiv Z^1 Z^3$, and applying the identity $(a - b)^{\otimes 3} = a^{\otimes 3} - 3a^{\otimes 2} \otimes b + 3a \otimes b^{\otimes 2} - b^{\otimes 3}$, and various rules of tensor products, we verify that the radial function is obtained as $f(r) = \langle \hat{V}, \rho^{\otimes 6} \rangle$ or explicitly as

$$\langle \hat{V}, \rho^{\otimes 6} \rangle = \langle \mathbb{I}^{\otimes 12} - 3Z^9 Z^{11} + 3Z^5 Z^7 Z^9 Z^{11} - Z^1 Z^3 Z^5 Z^7 Z^9 Z^{11}, \rho^{\otimes 6} \rangle.$$

The following decomposing of volume operator will be useful: $\widehat{V} = \sum_{a=1}^4 \lambda_a \widehat{V}_a$, with $\lambda = (\lambda_a)_{a=1}^4 = (1, -3, 3, -1)$, and the obvious identifications

$$\begin{aligned} \widehat{V}_1 &= \mathbb{I}^{\otimes 12}, \\ \widehat{V}_2 &= Z^9 Z^{11}, \\ \widehat{V}_3 &= Z^5 Z^7 Z^9 Z^{11}, \\ \widehat{V}_4 &= Z^1 Z^3 Z^5 Z^7 Z^9 Z^{11}, \end{aligned} \tag{5}$$

where each operator satisfies the properties of being an involution, unitary and Hermitian i.e., $\widehat{V}_a^2 = \mathbb{I}^{\otimes 12}$, $\widehat{V}_a^\dagger = \widehat{V}_a$.

Then, finally function $f(r)$ is expressed as

$$f(r) = \langle \widehat{V}, \rho^{\otimes 6} \rangle = \langle \widehat{V}_1, \rho^{\otimes 6} \rangle - 3 \langle \widehat{V}_2, \rho^{\otimes 6} \rangle + 3 \langle \widehat{V}_3, \rho^{\otimes 6} \rangle - \langle \widehat{V}_4, \rho^{\otimes 6} \rangle.$$

Further properties concerning the graph structure of the volume operator have been placed at the end of paper in Appendix C entitled: *Hypergraphs and volume operator*.

3. CZ Gates, Volume Observables and Function

Chapter’s outline: The aim of this central chapter is to provide the first operational algorithm of the separability probability distribution. To this end, all background material (cf. shifted CZ gates Hankel, Toeplitz, Fourier, Hadamard matrices and their interrelations), as well as relevant concepts and definitions, are introduced in order to establish the relation $f(r) = \langle \widehat{V}, \rho^{\otimes 6} \rangle = \langle \mathcal{R}(U^{cz}), \rho^{\otimes 6} \rangle = \langle U^{cz}, \mathcal{R}^*(\rho^{\otimes 6}) \rangle$. This relation describes the fact that the volume function is obtained as an expectation value of the volume observable, which in turn is shown to be derived from a unitary map \mathcal{R} or its dual map \mathcal{R}^* .

Preliminaries: Let the projectors $P_k = |k\rangle \langle k|$, $k \in [N]$, where $[N] = \{1, 2, \dots, N = 2^n\}$, in \mathbb{C}^N space. Denote by $k = (k_1, \dots, k_n)$, and $l = (l_1, \dots, l_n)$ the decimal and binary decomposition of indices $k, l \in \Lambda$, where $\Lambda \equiv \{0, 1\}^n$, and by $k \cdot l = k_1 l_1 + \dots + k_n l_n$ and $k + l = (k_1 + l_1, \dots, k_n + l_n)$, their *mod2* element-wise inner product and sum, respectively.

Let $|k\rangle = \otimes_{l=1}^n |k_l\rangle$ and consider the projectors $P_{k_l} = |k_l\rangle \langle k_l| = \frac{1}{2}(\mathbb{I} + (-1)^{k_l} Z)$. The reference controlled-phase gate CZ gate $U^{cz} = e^{i\pi P}$, uses the projector $P_{k=N-1} \equiv P$, acts on the space of n qubits and is labelled by n -plet of binary indices $(k_1 = 1, \dots, k_n = 1)$. For general index $k \in [N]$, the CZ gate operator $U_k^{cz} = e^{i\pi P_k}$ can be considered to act in multi-qubit states as follows:

$$U_k^{cz} |k_1, \dots, k_{n-1}, k_n\rangle = (-1)^{k_1 \dots k_n} |k_1, \dots, k_{n-1}, k_n\rangle.$$

States $|k_1, \dots, k_{n-1}\rangle$ may be regarded as control qubit states and $|k_n\rangle$ as the target qubit state, so the gate’s action is determined by the choice of values $k_i = 1, i = 1, \dots, n$.

To allow for free choice of the values of the n -plet index on which the conditional $e^{i\pi} = -1$ phase will be acted in a CZ gate, we need to introduce first the set of so-called *X-shifted CZ gates*. This is done in the proposition below where the family \mathcal{F}_k^{cz} of N commuting *X-shifted CZ gates* U_{k+l}^{cz} are defined. Shifted CZ are related linearly to words Z^m and vice versa, so volume operators \widehat{V}_a and \widehat{V} via their linear relation to Z^m words, Equation (5), are in turn related to shifted CZ gates.

The proposition proceeds by showing that all shifted CZ gates U_{k+l}^{cz} are generated via a unitary channel map \mathcal{R} , from the reference gate U^{cz} . This allows for expressing volume operators $\widehat{V}_a, \widehat{V}$ via map \mathcal{R} acting on U^{cz} , which is then trace contracted with a state density matrix i.e., $f(r) = \langle \mathcal{R}(U^{cz}), \rho^{\otimes 6} \rangle$, to provide the targeted volume function. By duality (defined precisely below), the volume function is obtained by operating with dual map \mathcal{R}^* on ρ instead with of \mathcal{R} acting on U^{cz} i.e., $f(r) = \langle M_1, \mathcal{R}^*(\rho^{\otimes 6}) \rangle$, where now the CZ gate has been identified with an operator observable i.e., $M_1 \equiv U^{cz}$. Hence, the volume function is obtained as the mean value of the quantum measurement

of the generalized observable M_1 , in state $\rho^{\otimes 6}$. This alternative way of evaluating volume functions strengthens the operational character of the process of dealing with volumes of separable states as a form of generalized quantum measurement.

We next proceed with the

Proposition 1. *The projection operators P_k and the words $Z^m \equiv Z^{m_1} \otimes \dots \otimes Z^{m_n}$ of letter Z are related by the Hadamard transform in the direct and the inverse way as $P_m = \frac{1}{N} \sum_{r \in \Lambda} (-1)^{m \cdot r} Z^r$ and $Z^m = \sum_{k \in \Lambda} (-1)^{m \cdot r} P_r$ for $r, m \in \Lambda$, respectively. From the CZ_k gates expressed as $U_k^{cz} = e^{i\pi P_k}$, the family of X-shifted CZ gates*

$$\mathcal{F}_k^{cz} \equiv \{U_{k+l}^{cz} = X^l U_k^{cz} (X^T)^l, l \in \Lambda\}$$

is generated by its members, which, in terms of projectors, read explicitly

$$U_{k+l}^{cz} = \sum_{m \in \Lambda} (-1)^{(k_1+l_1+m_1+1) \dots (k_n+l_n+m_n+1)} P_{m_1 \dots m_n}.$$

The effect of index shifting ($k \rightarrow k+l$) on gates is to allow a conditional placing of a minus sign at position $k+l \in \Lambda$; as a consequence, shifted gates have the spectral decomposition

$$U_{k+l}^{cz} = -|k+l\rangle \langle k+l| + \sum_{m \in \Lambda \setminus \{k+l\}} |m\rangle \langle m|.$$

For zero shift $l = 0$ and $k = N - 1$, the gate $U_{N-1+0}^{cz} \equiv U^{cz}$ is identified with the usual CZ gate in the computational basis. Shifted CZ gates are linearly related to words Z^r as

$$U_{k+l}^{cz} = \sum_{r \in \Lambda} C_{k+l,r} Z^r,$$

via the orthogonal matrix $C = AH$, where the product is between Hankel A and Hadamard H matrices and the C matrix elements explicitly read

$$C_{k+l,r} = (AH)_{k+l,r} = \frac{1}{2^n} \sum_{m \in \Lambda} (-1)^{(k_1+l_1+m_1+1) \dots (k_n+l_n+m_n+1) + m_1 r_1 + \dots + m_n r_n}.$$

Conversely the $Z^r, r \in \Lambda$, words relate to the CZ shifted gates as

$$Z^r = \sum_{k+l \in \Lambda} C_{k+l,r}^\dagger U_{k+l}^{cz}.$$

This in turn, by virtue of Equation (5), allows the volume operators $\{\widehat{V}_a = Z^{l_a}; a \in \{1, 2, 3, 4\}, l_a = \{l_{a_m}\}_{m=1}^n\}$, to be expressed in terms of CZ gates

$$\widehat{V}_a = \sum_{k+l \in \Lambda} C_{k+l,l_a}^\dagger U_{k+l}^{cz}. \tag{6}$$

A further reduction results by first generating each and all of the components $\widehat{V}_a, a = 1, 2, 3, 4$, of volume operator from the single reference gate U^{cz} via the action $U^{cz} \rightarrow \widehat{V}_a = \mathcal{R}_a(U^{cz})$, of unitary maps \mathcal{R}_a which are defined as

$$T \rightarrow \mathcal{R}_a(T) := \sum_{k+l \in \Lambda} C_{k+l,l_a}^\dagger X^{k+l+1} T X^{k+l+1}.$$

Explicitly, the volume operators $\widehat{V}_a = Z^{l_a} \equiv Z^{l_{a_1}} \otimes \dots \otimes Z^{l_{a_n}}$ are described by using the labelling map $a \rightarrow l_a = (l_{a_1}, l_{a_2}, \dots, l_{a_n})$, which leads to the following four index correspondences for each one of them (only the non zero l_{a_i} 's are provided): For $\widehat{V}_1 = \mathbb{I}, \{l_{1_m} = 0\}_{m=1}^n$; for \widehat{V}_2 , the non zero components are $l_{2_1=9} = l_{2_2=11} = 1$;

for \widehat{V}_3 , the non zero indices are $l_{3_1=5} = l_{3_2=7} = l_{3_3=9} = l_{3_4=11} = 1$, and finally, for \widehat{V}_4 , the non zero indices are $l_{4_1=1} = l_{4_2=3} = l_{4_3=5} = l_{4_4=7} = l_{4_5=9} = l_{4_6=11} = 1$.

The total volume operator \widehat{V} is eventually obtained via the action of map $\mathcal{R} : \mathbb{C}^{N \times N} \rightarrow \mathbb{C}^{N \times N}$ on the reference gate, i.e., $\widehat{V} =: \mathcal{R}(U^{cz})$, where map \mathcal{R} is a weighted sum of \mathcal{R}_a maps, which explicitly reads $T \rightarrow \mathcal{R}(T) := \sum_{a=1}^4 \lambda_a \mathcal{R}_a(T)$, with weights $\lambda = (\lambda_a)_{a=1}^4 = (1, -3, 3, -1)$.

By means of the later result and the previous identification $M_1 \equiv U^{cz}$, the evaluation of volume function $f(r)$ is cast in the suggestive form

$$f(r) = \langle \mathcal{R}(U^{cz}), \rho^{\otimes 6} \rangle = \langle U^{cz}, \mathcal{R}^*(\rho^{\otimes 6}) \rangle = \langle M_1, \rho_1 \rangle \equiv \langle M_1 \rangle_{\rho_1}, \tag{7}$$

where $\rho_1 \equiv \mathcal{R}^*(\rho^{\otimes 6})$ and map \mathcal{R}^* the dual of \mathcal{R} has been utilized.

Finally, via the expression $U^{cz} = \mathbb{I} - 2P_{N-1} = P_{N-1}^\dagger - P_{N-1}$ of CZ gate, the volume function evaluates to

$$f(r) = \sum_{a=1}^4 \lambda_a \{ \text{Tr}[\mathcal{R}_a^*(\rho^{\otimes 6})] - 2 \langle N-1 | \mathcal{R}_a^*(\rho^{\otimes 6}) | N-1 \rangle \}. \tag{8}$$

The proof is deferred to Appendix A.

4. Hypergraph Hamiltonian Coupling

Chapter's outline: The aim of this chapter is to provide the second operational algorithm of the separability probability distribution. This volumetric radial distribution is shown to be expressed by means of the expectation value of a quantum observable M_2 on an appropriate state. This state is a U evolved density matrix describing a multiple of copies of X states. The Hamiltonian H_V generating unitary U and its hypergraph coupling structure are determined.

The preceding analysis will be utilized to provide an operational implementation of the volume function $\langle \widehat{V}_{I_a}, \rho^{\otimes 6} \rangle$ via a unitary operator $U \equiv e^{iH_V}$ and its generating Hamiltonian H_V , both acting in an extended Hilbert space to that of the density matrix of the 12 qubits, as follows: Let us first introduce the conditional unitary operator

$$U = \sum_{a=1}^4 P_a \otimes \widehat{V}_a, \tag{9}$$

and an auxiliary density matrix ρ_{aux} acting on an auxiliary 2-qubit Hilbert space $H_{aux} \approx \mathbb{C}^4$. The initial composite system density matrix $\rho_{aux} \otimes \rho^{\otimes 6}$ evolves as

$$\rho_{aux} \otimes \rho^{\otimes 6} \rightarrow U \rho_{aux} \otimes \rho^{\otimes 6} U^\dagger \equiv \rho_2.$$

Next, introduce the correlating observable

$$M_2 = \sum_{b=1}^4 \mu_b P_b \otimes \widehat{V}_b, \tag{10}$$

where the real coefficient $\mu = (\mu_a)_{a=1}^4$ should be determined.

Performing the *volumetric quantum measurement via* M_2 on the evolved state ρ_2 , we demand that the mean value of the measurement equals the volume function i.e.,

$$\langle M_2 \rangle_{\rho_2} \equiv \langle M_2, \rho_2 \rangle = \text{Tr}(M_2 \rho_2) = f(r). \tag{11}$$

This is achieved by choosing values for the diagonal elements of the auxiliary density matrix ρ_1 to be the probabilities $p = (p_a = \langle a | \rho_{aux} | a \rangle)_{a=1}^4$, which together with the terms of the sequence μ should

satisfy the constraint $(p_a \mu_a)_{a=1}^4 = (1, -3, 3, -1)$. A possible choice for p is the uniform distribution i.e., $p_a = \frac{1}{4}$ and for the coefficients $\mu = (\mu_a)_{a=1}^4 = (4, -12, 12, -4) = 4\lambda$.

Furthermore, modifying numerically observable M_2 into $M_{HS}^{(X)} \equiv \frac{2\pi^2}{9} M_2$ and $M_{HS,sep}^{(X)} \equiv \frac{4\pi^2}{45} M_2$, yields the exact results of the volumetric quantum measurements of these operators respectively as

$$\begin{aligned} \langle M_{HS}^{(X)} \rangle &\equiv \text{Tr}(M_{HS}^{(X)} \cdot \rho_2) = V_{HS}^{(X)}(r), \\ \langle M_{HS,sep}^{(X)} \rangle &\equiv \text{Tr}(M_{HS,sep}^{(X)} \cdot \rho_2) = V_{HS,sep}^{(X)}(r), \end{aligned}$$

from which the probability distribution of the radial parameter is finally obtained i.e., $p_{sep}^{(X)}(r) = \frac{\langle M_{HS}^{(X)} \rangle}{\langle M_{HS,sep}^{(X)} \rangle} = \frac{2}{5}, r \in [0, 1)$.

Next, we determine the Hamiltonian H_V that generates the unitary U as $U = e^{iH_V}$ by invoking the identity,

$$\exp\left(-\frac{i\pi}{2}(2r+1)(Z^{j_1} \otimes Z^{j_2} \otimes \dots \otimes Z^{j_n} - \mathbb{I}_{2^n})\right) = Z^{j_1} \otimes Z^{j_2} \otimes \dots \otimes Z^{j_n},$$

valid for $r \in \mathbb{Z}$, $j_i = 0, x, y, z$, (where $Z_0 \equiv \mathbb{I}$) [32], from which equivalent expressions for V_a 's are obtained i.e., $\hat{V}_{l_a} = Z^{l_a} = e^{-\frac{i\pi}{2}(2r+1)Z^{l_a}}$, from which we choose $\hat{V}_{l_a} = e^{\frac{i\pi}{2}l_a}$. Then, the multi-spin Hamiltonian generator $H_V = \sum_{a=1}^4 P_a \otimes \hat{V}_a$ of U , i.e., $U \equiv e^{iH_V}$, reads explicitly

$$H_V = \frac{\pi}{2}(P_1 \otimes \mathbb{I}^{\otimes 12} + P_2 \otimes Z^9 Z^{11} + P_3 \otimes Z^5 Z^7 Z^9 Z^{11} + P_4 \otimes Z^1 Z^3 Z^5 Z^7 Z^9 Z^{11}). \tag{12}$$

Referring to Appendix C: *Hypergraphs and volume operator*, we see that, similarly to the hypergraph structure of the volume operator, the resulting effective Hamiltonian operator of this chapter shares a similar hypergraph structure.

5. Quantum Walk Simulation of Separability

Chapter's outline: The aim of this chapter is to provide the third and final operational algorithm of the separability probability distribution. To this end, a QW set up with quantum coin and walker systems is employed. Volume function is again obtained via a quantum measurement of a multi-qubit observable on a state that results after evolving an initial X density matrix with a conditional completely positive trace preserving (CPTP) map of the QW type. Decomposition of QW map into a CP map with volume operators as Kraus generators' time local unitaries is provided. An overall comment comparing the three schemes generating separability statistics is provided.

Measurement theory: The quantum measurement content of the QW-based operational algorithm of separability statistics to be presented follows the generalized theory of quantum measurement. A brief outline of this theory follows: on a quantum system S in state ρ , a measurement is described by a (POVM) positive operator valued measure $\{Q_k\}_k$. Each outcome indexed by k occurs with probability $p_k = \text{Tr}(Q_k \rho)$. The completely positive trace preserving map associated with the measurement reads

$$\rho \rightarrow \mathcal{D}(\rho) = \sum_k |k\rangle \langle k|_C \otimes \mathcal{D}^{(k)}(\rho),$$

where C is a classical register (measuring device) that contains the outcomes of the measurement and

$$\mathcal{D}^{(k)}(\rho) = \sum_i S_i^{(k)}(\rho) S_i^{(k)\dagger}$$

is the post-measurement state of the initial ρ corresponding to outcome k . This post-measurement state is induced by a CPTP (completely positive trace preserving) map $\mathcal{D}^{(k)}$, generated by its Kraus

generators $\{S_i^{(k)}\}_i$, which in turn generate the POVM elements as $Q_k = \sum_i S_i^{(k)\dagger} S_i^{(k)}$. The trace preservation of map \mathcal{D} leads to the completeness of the POVM set i.e. $\sum_k Q_k = \mathbb{I}$. Note that this scheme does not assume projectivity of each or orthogonality of different Q 's, so it is a generalization of the von Neumann projection measurement theory, in which special case the additional relations $Q_k^2 = Q_k$ for all k 's are valid; see, e.g., [25].

The algorithm: An alternative QW based simulation of the volume function can be given by constructing a new state ρ_2 in place of ρ_1 of the preceding analysis, and also by replacing the unitary U acting in $\mathbb{C}^4 \otimes \mathbb{C}^{2^{12}}$, by the extended unitary operator W acting in $\mathbb{C}^4 \otimes \mathbb{C}^2 \otimes \mathbb{C}^{2^{12}}$. The three state spaces correspond respectively to the states for the auxiliary system, the coin system and the 'walker' target system to which an intentional action is aimed.

Consider first the unitary operator

$$W = \sum_{a=1}^4 P_a \otimes W_a,$$

where W_a are unitary step operators for a quantum walk, as will be detailed below, written as

$$W_a = (P'_0 \otimes \mathbb{I} + P'_1 \otimes \widehat{V}_a)(H \otimes \mathbb{I}) = \frac{1}{\sqrt{2}} \begin{pmatrix} \mathbb{I} & \mathbb{I} \\ \widehat{V}_a & -\widehat{V}_a \end{pmatrix}.$$

Then, we compute \mathcal{E}_a , the evolution unitary CP map for the a -th QW, where we choose the initial coin state to be $\rho_c = |1\rangle\langle 1|$, as follows:

$$\begin{aligned} Tr_c[W_a(\rho_c \otimes \rho^{\otimes 6})W_a^\dagger] &= \frac{1}{2} Tr_c \begin{pmatrix} \mathbb{I} & \mathbb{I} \\ \widehat{V}_a & -\widehat{V}_a \end{pmatrix} \begin{pmatrix} 0 & 0 \\ 0 & \rho^{\otimes 6} \end{pmatrix} \begin{pmatrix} \mathbb{I} & \widehat{V}_a^\dagger \\ \mathbb{I} & -\widehat{V}_a^\dagger \end{pmatrix} \\ &= \frac{1}{2}(\rho^{\otimes 6} + \widehat{V}_a \rho^{\otimes 6} \widehat{V}_a^\dagger) \equiv \mathcal{E}_a(\rho^{\otimes 6}). \end{aligned}$$

Explicit computation of the total action of the unitary W generates, after partial tracing of the coin system, the QW CP map \mathcal{E}_{qw} that eventually yields the target density matrix ρ_2 , as follows ($\rho_{aux} = \frac{1}{4}\mathbb{I}$):

$$\begin{aligned} \mathcal{E}_{qw}(\rho^{\otimes 6}) &\equiv Tr_c W(\rho_{aux} \otimes \rho_c \otimes \rho^{\otimes 6})W^\dagger = Tr_c \sum_{a=1}^4 \sum_{b=1}^4 (P_a \otimes W_a)(\rho_{aux} \otimes \rho_c \otimes \rho^{\otimes 6})(P_b \otimes W_b^\dagger) \\ &= Tr_c \sum_{a=1}^4 \sum_{b=1}^4 \left(\frac{1}{4} P_a \mathbb{I} P_b \otimes W_a(\rho_c \otimes \rho^{\otimes 6})W_b^\dagger\right) \\ &= \sum_{a=1}^4 \frac{1}{4} P_a \otimes \frac{1}{2}(\rho^{\otimes 6} + V_a \rho^{\otimes 6} V_a^\dagger) \equiv \frac{1}{4} \sum_{a=1}^4 P_a \otimes \mathcal{E}_a(\rho^{\otimes 6}) \equiv \rho_3. \end{aligned} \tag{13}$$

In the next and final step, we reach the volume function via quantum measurement with the observable $M_3 = 2 \sum_{b=1}^4 \lambda_b P_b \otimes \widehat{V}_b$, in the state ρ_3 as $Tr(M_3 \rho_3) = \langle M_3, \rho_3 \rangle = f(r) \equiv \langle M_3 \rangle_{\rho_3}$. Indeed,

$$\begin{aligned}
 \text{Tr}(M_3\rho_3) &= \frac{1}{4}2\text{Tr} \sum_{a=1}^4 \sum_{b=1}^4 \lambda_b P_a P_b \otimes \widehat{V}_b \mathcal{E}_a(\rho^{\otimes 6}) = \frac{1}{2} \sum_{a=1}^4 \lambda_a \text{Tr}(\widehat{V}_b \mathcal{E}_a(\rho^{\otimes 6})) \\
 &= \frac{1}{2} \sum_{a=1}^4 \lambda_a \text{Tr}(\widehat{V}_b (\frac{1}{2}(\rho^{\otimes 6} + \widehat{V}_a \rho^{\otimes 6} \widehat{V}_a^\dagger))) \\
 &= \frac{1}{4} \sum_{a=1}^4 \lambda_a \text{Tr}(\widehat{V}_b \rho^{\otimes 6}) + \frac{1}{4} \sum_{a=1}^4 \lambda_a \text{Tr}(\widehat{V}_b \widehat{V}_a \rho^{\otimes 6} \widehat{V}_a^\dagger) \\
 &= \frac{1}{2} \langle \rho^{\otimes 6}, \widehat{V} \rangle + \frac{1}{2} \langle \rho^{\otimes 6}, \widehat{V} \rangle \\
 &= \langle M_3, \rho_3 \rangle \equiv \langle M_3 \rangle_{\rho_3} = f(r).
 \end{aligned}
 \tag{14}$$

Elaborating further on this QW-based alternative, we note that the observable M_3 is a form of controlled-phase operator and can be expressed equivalently as

$$M_3 = \begin{pmatrix} 2\mathbb{I}^{\otimes 12} & & & \\ & -6\mathbb{I}^{\otimes 8} \otimes (Z \otimes \mathbb{I})^{\otimes 2} & & \\ & & 6\mathbb{I}^{\otimes 4} \otimes (Z \otimes \mathbb{I})^{\otimes 4} & \\ & & & -2(Z \otimes \mathbb{I})^{\otimes 6} \end{pmatrix}.$$

Referring to density matrix ρ_3 , we re-express the QW CP maps $\mathcal{E}_2, \mathcal{E}_3, \mathcal{E}_4$ in terms of only one of them i.e., of $\mathcal{E}_2 \equiv \mathcal{E}$, which we recall here

$$\mathcal{E}(\rho^{\otimes 6}) = \frac{1}{2}(\rho^{\otimes 6} + (Z^9 Z^{11})\rho^{\otimes 6}(Z^9 Z^{11})^\dagger) \equiv \tilde{\rho}_3.
 \tag{15}$$

Note that $\tilde{\rho}_3$ is an intermediate form of the initial multi X-state density matrix that will be transformed further until its final target form. However, first let us establish the property of expressing maps $\mathcal{E}_3, \mathcal{E}_4$ from \mathcal{E}_2 . To this end, observe that

$$\widehat{V}_2 \xrightarrow{Z^5 Z^7} \widehat{V}_3 \xrightarrow{Z^1 Z^3} \widehat{V}_4,$$

i.e., the unitary \widehat{V}_2 can generate the two other unitary operators by appropriate multiplications. Since the generators of the maps $\mathcal{E}_2, \mathcal{E}_3, \mathcal{E}_4$ are given in terms of the \widehat{V}_i 's, it follows from the last equation above that only the CP map $\mathcal{E}_2 \equiv \mathcal{E}$ with its Kraus generators $\{\mathbb{I}, Z^9 Z^{11}\}$ needs be considered. This is so since the rest maps can be generated via local unitary transformation using local Z 's as the following scheme indicates

$$\begin{aligned}
 \mathcal{E}_1 &= \rho^{\otimes 6}, \\
 \mathcal{E}_2 &= \mathcal{E}(\rho^{\otimes 6}), \\
 \mathcal{E}_3 &= (Z^5 Z^7) \circ \mathcal{E}(\rho^{\otimes 6}) \circ (Z^5 Z^7)^\dagger, \\
 \mathcal{E}_4 &= (Z^1 Z^3 Z^5 Z^7) \circ \mathcal{E}(\rho^{\otimes 6}) \circ (Z^1 Z^3 Z^5 Z^7)^\dagger.
 \end{aligned}$$

This result eventually allows for re-expressing the target density matrix $\mathcal{E}_{qw}(\rho^{\otimes 6}) \equiv \rho_3$ in the following suggestive way:

$$\begin{aligned} \rho_3 &= \frac{1}{4} \begin{pmatrix} \rho^{\otimes 6} & & & \\ & \mathcal{E}_2(\rho^{\otimes 6}) & & \\ & & \mathcal{E}_3(\rho^{\otimes 6}) & \\ & & & \mathcal{E}_4(\rho^{\otimes 6}) \end{pmatrix} \\ &= \frac{1}{4} \begin{pmatrix} \mathbb{I}_{4^6} & & & \\ & \mathbb{I}_{4^6} & & \\ & & Z^5 Z^7 & \\ & & & Z^1 Z^3 Z^5 Z^7 \end{pmatrix} \mathbb{I}_4 \otimes \tilde{\rho}_3 \begin{pmatrix} \mathbb{I}_{4^6} & & & \\ & \mathbb{I}_{4^6} & & \\ & & Z^5 Z^7 & \\ & & & Z^1 Z^3 Z^5 Z^7 \end{pmatrix}^\dagger. \end{aligned}$$

Factorizing the construction of density matrix ρ_3 , into a single two body CP map, cf. Equation (15), times local actions of Z matrices, reduces considerably the required resources for this operational approach to separability statistics.

Final comment: Summarizing the results of this and the previous two chapters, we see that the volume function has been obtained via quantum measurements respectively of the multi-qubit observables M_1, M_2 and M_3 in the respected states given by the density matrices ρ_1, ρ_2 and ρ_3 according to the following scheme $f(r) = \text{Tr}(M_1 \rho_1) = \text{Tr}(M_2 \rho_2) = \text{Tr}(M_3 \rho_3)$, cf. Equations (7), (11) and (14). These states have been generated from the given separable X-states via either a multi-qubit X map, or by a Hamiltonian generated unitary action or alternatively by a unitary CP map of the QW type combined with additional local unitary actions. The three algorithms are based on the underlying hypergraph coupling structure of the 12-qubit lattice system that generates the measuring states $\rho_{1,2,3}$. Though explicit mention of hypergraph state generation has not been made in this work, a more detailed analysis (not to be presented here) would reveal the role of hypergraph state quantum entanglement for the operational algorithms. Finally, the operational scheme put forward here is general enough to enable simulation of other distributions of radial functions beyond those employed in the question of separability statistics. Such other applications would be referred to Appendix B dealing with generalizations of the present approach.

6. Aspects of Computation and Implementation

Chapter's outline: Relations regarding the presented operational approach to separability and the computation via IQP circuits are discussed in addition to possible connections to LHZ implementation architecture are provided.

Computation: Instantaneous Quantum Polynomial-time Computing (IQP) is a type of universal computation that utilizes quantum circuits made of gates that are diagonal in the Z-basis while the input–output states are usually X-basis states and results are obtained by measurements in this basis [14–21]. CZ gates embedded in multi-qubit spaces are the main building blocks of these circuits, the commutativity of which allows their implementation to be performed simultaneously or in any other time order, hence the name of IQP. The Hamiltonian dynamics generating such states would require little control over the time ordering of multiple-qubit interactions needed, hence rendering the physical implementation to more robust to errors. Further IQP circuits being diagonal are more robust to quantum noise than the off diagonal circuits are to decoherence, hence they hold an additional merit. Finally, diagonal gates are fault-tolerantly realizable by current technology e.g., in superconducting and semiconducting systems. Despite these advantages, IQP circuits have been applied to a limited number of applications e.g., to the random states generation and to hypergraph state entanglement. The present work is a novel application of diagonal circuits that combine hypergraph structures and operational methods for crafting states that their appropriate sampling would generate the elusive statistics of separable bipartite qubit systems in the X state. Some important questions regarding the

potential advantage of quantum sampling over classical sampling would be addressed in the present operational framework concerning separable states, however, they fall outside the scope of this paper.

Implementation: Recent developments in physical implementation of higher order interactions of systems that encode quantum qubits have resulted into a well-developed quantum simulation toolbox involving Rydberg atoms, known as the Lechner–Hauke–Zoller (LHZ) architecture [22,23]. The set up allows one to build a prototype for a coherent adiabatic model with all-to-all Ising type interactions and therefore to provide a platform for realization of two, three, four-body and higher order interactions. The architecture can be physically realized on various physical platforms with local controllability, including cases such as superconducting qubits, NV-centers, quantum dots, and atomic systems. The 12-qubit lattice model of this work, implementing states and measurements that would simulate separable states would be an interesting problem to address within the LHZ architecture.

7. Conclusions

Quantum separability of multi-qubit states has been investigated in this work by devising operational ways to verify the statistics of the phenomenon. The algorithms suggested use generalized measurement theory and unitary in addition to non-unitary CP transformation in order to prepare the X states, the special type of separable states under study, for quantum measurement that would yield outcomes simulating separability statistics. Possible connections of the present formalism to the computational methodology with diagonal quantum circuits as well as to some main implementation architecture have been outlined. One out of the possible generalizations and ramifications of this work is worth being selected for a closing discussion topic. It has been clear from the methodology developed so far that polynomial functions of Bloch vector components could be the resulting functions of designed generalized quantum measurements of some new observables that would in turn require some designed transformation applied on initial X state density matrices. This line of investigation seems rather useful and would be developed to a tool that trades tensoring of multi-qubit states to polynomial and maybe analytic functions of Bloch vector components treated as independent variables. We aim to return to this point elsewhere.

Funding: This research received no external funding.

Acknowledgments: I am grateful to D. Angelakis for his generous hospitality at the Centre for Quantum Technologies, Singapore, where part of this work was carried out, and for discussions. I also acknowledge discussions with A. Winter and D. Petrosyan. The work was done partially while the author was visiting the Institute for Mathematical Sciences, National University of Singapore in 2017. Some preliminary versions of this work were presented as a poster in the Conference “Beyond I.I.D. in Information Theory”, 2017, in Singapore and as a talk in the “Workshop on Quantum Matter” in SigmaPhi2017–International Conference in Corfu.

Conflicts of Interest: The author declares no conflict of interest.

Appendix A. Hankel, Toeplitz, Fourier, Hadamard, CZ and Volume Matrices

Projectors P and Z operators: Let the projector $P_k = |k\rangle \langle k|$, $k = 1, 2, 3, 4$, in \mathbb{C}^4 space, then let $k = 1 + k_1 2^0 + k_2 2^1$, $k_i = 0, 1$, and decompose P_k into product of projectors in two qubit spaces \mathbb{C}^2 ,

$$\begin{aligned} P_k &= Q_{k_2} \otimes Q_{k_1} = \frac{\mathbb{I} + (-1)^{k_2} Z}{2} \otimes \frac{\mathbb{I} + (-1)^{k_1} Z}{2} \\ &= \frac{1}{4} \left(\mathbb{I} \otimes \mathbb{I} + (-1)^{k_1} \mathbb{I} \otimes Z + (-1)^{k_2} Z \otimes \mathbb{I} + (-1)^{k_1+k_2} Z \otimes Z \right). \end{aligned}$$

Generalizing this decomposition to projectors $P_k = |k\rangle \langle k|, k = 1, \dots, N$, in \mathbb{C}^N , the state space of an N -dimensional system i.e., the state space of n qubits, we consider the binary decomposition $k = 1 + k_1 2^0 + k_2 2^1 \dots + k_n 2^{n-1}, k_i = 0, 1$, and decompose the general projection as

$$\begin{aligned}
 P_k &= \bigotimes_{l=1}^n Q_{k_l} = \frac{1}{N} \bigotimes_{l=1}^n (\mathbb{I} + (-1)^{k_l} Z) \\
 &= |k_1\rangle \langle k_1| \otimes \dots \otimes |k_n\rangle \langle k_n|.
 \end{aligned}
 \tag{A1}$$

A compact relation in terms of the Fourier transform exists between the projectors P_k and products of qubit Pauli matrices which can be obtained by first writing the case $n = 2$ for motivation as follows:

$$P_k = \frac{1}{2^2} \sum_{l_1, l_2=0,1} (-1)^{k_1 l_1 + k_2 l_2} Z^{l_2} \otimes Z^{l_1},$$

then the general case reads

$$P_k = \frac{1}{N} \sum_{l \in \{0,1\}^n} (-1)^{k_1 l_1 + \dots + k_n l_n} Z^{l_1} \otimes Z^{l_2} \otimes \dots \otimes Z^{l_n}.
 \tag{A2}$$

Further denoting by $k = (k_1, \dots, k_n)$, and $l = (l_1, \dots, l_n)$, the decimal and binary decomposition of indices k, l , and $\Lambda \equiv \{0, 1\}^n$ so $k, l \in \Lambda$, and by $k \cdot l = k_1 l_1 + \dots + k_n l_n \pmod{2}$, their inner product, as well as using the symbol/word $Z^l \equiv Z^{l_1} \otimes Z^{l_2} \otimes \dots \otimes Z^{l_n}$, we find for projectors the relation

$$P_k = \frac{1}{N} \sum_{l \in \Lambda} (-1)^{k \cdot l} Z^l.
 \tag{A3}$$

This is identified with the finite Fourier transform i.e., $P_k = \sum_l H_{kl} Z^l$, where $H_{kl} = \frac{1}{N} (-1)^{k \cdot l} = \frac{1}{N} (e^{i\pi})^{k \cdot l}$ stands for the elements of the Hadamard transform unitary matrix (this is also identified with finite Fourier transform matrix $F_{k,l}(\phi) = \frac{1}{N} e^{i\phi k \cdot l} \in \mathbb{C}^{N \times N}$, for the choice $\phi = \pi$).

Hence, the inverse relation follows from the expressions

$$\sum_{k \in \Lambda} (-1)^{k \cdot l} P_k = \frac{1}{N} \sum_{k \in \Lambda} \sum_{l' \in \Lambda} (-1)^{k \cdot l} (-1)^{k \cdot l'} Z^{l'} = Z^l,$$

where the relation $\sum_{k \in \Lambda} (-1)^{k \cdot (l+l')} = \frac{1}{N} \delta_{ll'}$, have been use. Then,

$$\begin{aligned}
 Z^l &= \sum_{k \in \Lambda} (-1)^{k \cdot l} P_k \\
 &= \sum_{k \in \Lambda} (-1)^{k \cdot l} |k_1\rangle \langle k_1| \otimes \dots \otimes |k_n\rangle \langle k_n|.
 \end{aligned}
 \tag{A4}$$

Control Z gates: The generalized controlled-Z phase gates can be obtained by exponentiation of projector $P_{k=N-1} \equiv P$, in the n qubits space i.e., $U^{cz} = e^{i\pi P}$, where by means of decimal-binary decomposition $k = (k_1, \dots, k_n)$ the choice $k = N - 1$ leads to $(k_1 = 1, \dots, k_n = 1)$.

By means of Equation (A3), the gate decomposes for a general index $k = (k_1, \dots, k_n)$ as

$$U_k^{cz} = \prod_{(l_1, \dots, l_n) \in \Lambda} e^{\frac{i\pi}{2^n} (-1)^{k_1 l_1 + \dots + k_n l_n} Z^{l_1} \otimes Z^{l_2} \otimes \dots \otimes Z^{l_n}},
 \tag{A5}$$

or concisely

$$U_k^{cz} = \prod_{l \in \Lambda} e^{\frac{i\pi}{2^n} (-1)^{k \cdot l} Z^l}.
 \tag{A6}$$

Note that via the decimal-binary decomposition $k = (k_1, \dots, k_n)$, the state vectors $|k\rangle \in \{|i\rangle\}_{i=1}^{2^n}$ labelled by k , are mapped uniquely to states of n qubits $|m_1, \dots, m_n\rangle \in \{|k_1, \dots, k_n\rangle\}_{(k_1, \dots, k_n) \in \Lambda}$, so that the gates CZ read in the multi-qubit representation

$$U_k^{cz} = \sum_{(k_1, \dots, k_n) \in \Lambda} (-1)^{k_1 \dots k_n} |k_1, \dots, k_{n-1}, k_n\rangle \langle k_1, \dots, k_{n-1}, k_n|. \tag{A7}$$

For example, states $|k_1, \dots, k_{n-1}\rangle$ control qubit state $|k_n\rangle$ which is denoted the target qubit state, and the action of the gate is determined by the choice $k_i = 1, i = 1, \dots, n$. Explicitly, the action reads $U_k^{cz} |1, \dots, 1, 1\rangle = -|1, \dots, 1, 1\rangle$, on state $|1, \dots, 1, 1\rangle$, and is identity on all other states.

Other choices for parameter $k \in \Lambda$ in U_k^{cz} except $k = (1, \dots, 1, 1)$ are also possible and in fact are indispensable, especially in the context of volume operators as will be clear subsequently.

An important generalization of CZ gates is the embedding of them in the matrix space $\mathbb{C}^{N \times N}$, which means that along some axes the operator acts trivially as the unit matrix. This implies that the gate U_k^{cz} is now labelled by the powerset $\mathcal{P}(\Lambda)$ of Λ i.e., $k \in \mathcal{P}(\Lambda)$.

We turn now to the proof of the Proposition in the main text.

Proof of Proposition 1. Firstly to address the question of relating volume operators to CZ gates embedded in $\mathbb{C}^{N \times N}$, we turn to some basic properties and relations among Hankel, Toeplitz, Fourier, Hadamard matrices, and CZ gates.

Recall first the definition of the following matrices in $\mathbb{C}^{N \times N}$: the Toeplitz matrix with elements $T_{ij} = a_{i-j}$, the Hankel matrix with elements $A_{ij} = a_{i+j}$, the Fourier matrix with elements $F_{ij} = \frac{1}{\sqrt{N}} \omega^{ij}$ where $\omega = e^{\frac{i2\pi}{N}}$, the Hadamard matrix with elements $H_{ij} = \frac{1}{\sqrt{N}} (-1)^{i \cdot j}$ and finally the reflection matrix with elements $J_{ij}^{(n)} = \delta_{i+j, n+1}$, and some of their properties: $A = TJ$, $J^2 = \mathbb{I}$, since $J^T = J$, and the Toeplitz matrices are unitary/symmetric i.e., $TT^T = \mathbb{I}$, then $A^T = J^T T^T$, so Hankel matrices are also symmetric i.e., $AA^T = TJJ^T = TT^T = \mathbb{I}$.

Define next the family of X -shifted CZ gates

$$\mathcal{F}_{cz} \equiv \{U_{k+l}^{cz} = X^l U_k^{cz} (X^T)^l, l \in \Lambda\},$$

with $XX^T = \mathbb{I}$, where $X^l \equiv \otimes_{i=1}^n X^{l_i}$ and $X^{l_i} = (1 - l_i)\mathbb{I} + l_i X$, i.e., $X^{l_i} |k_i\rangle = (1 - l_i) |k_i\rangle + l_i |k_i + 1\rangle$.

In addition, note that $|\mathcal{F}_{cz}| = |\Lambda| = |\{0, 1\}^n| = N$. Explicitly for $l \equiv (l_i)_{i=1}^n$, $k \equiv (k_i)_{i=1}^n$, $k, l \in \Lambda$, so all CZ gates for n qubits read $U_{k+l}^{cz} = X^l e^{i\pi P_k} (X^T)^l = X^l U_k^{cz} (X^T)^l$, or explicitly

$$U_{k+l}^{cz} = \sum_{m \in \Lambda} (-1)^{(k_1+l_1+m_1+1) \dots (k_n+l_n+m_n+1)} P_{m_1 \dots m_n}. \tag{A8}$$

Recall also that $P_{k_1 k_2 \dots k_n} = \otimes_{j=1}^n |k_j\rangle \langle k_j|$ and that $P_k = \sum_{l \in \Lambda} H_{kl} Z^l$, where H_{kl} be the Hadamard matrix. Define next the Hankel matrix A with elements

$$A_{lk} = (-1)^{(l_1+k_1)(l_2+k_2) \dots (l_n+k_n)},$$

and its transpose

$$A_{lk}^T = \frac{1}{2^n} (-1)^{(l_1+k_1)(l_2+k_2) \dots (l_n+k_n)}.$$

Referring to Equation (A8), we have

$$U_{k+l}^{cz} = \sum_{m \in \Lambda} A_{k+l, m} P_m = \sum_{r \in \Lambda} \left(\sum_{m \in \Lambda} A_{k+l, m} H_{mr} \right) Z^r = \sum_{r \in \Lambda} (AH)_{k+l, r} Z^r,$$

or explicitly

$$U_{k+l}^{cz} = \frac{1}{2^n} \sum_{m \in \Lambda} (-1)^{(k_1+l_1+m_1+1) \cdots (k_n+l_n+m_n+1)+m_1r_1+\cdots+m_nr_n} Z^m. \quad (A9)$$

Defining the orthogonal matrix $C = AH$, with property $C^T C = (AH)^T AH = H^T A^T AH = \mathbb{I}$, and elements

$$C_{k+l,r} = (AH)_{k+l,r} = \frac{1}{2^n} \sum_{m \in \Lambda} (-1)^{(k_1+l_1+m_1+1) \cdots (k_n+l_n+m_n+1)+m_1r_1+\cdots+m_nr_n},$$

we arrive at the direct relation

$$U_{k+l}^{cz} = \sum_{r \in \Lambda} C_{k+l,r} Z^r, \quad (A10)$$

and its inverse

$$Z^r = \sum_{k+l \in \Lambda} C_{k+l,r}^\dagger U_{k+l}^{cz}. \quad (A11)$$

Volume operators: Turn now to the special case of a fixed n and to the binary n -plets and some subset of labels e.g., $l_a \equiv \{l_{a_1}, l_{a_2}, \dots, l_{a_{2m}}\}$ with indices $2m < n$. e.g., consider $n = 12$, then the volume operators are cast in form $\widehat{V}_{l_a} = Z^{l_a}$, cf. Equation (5). Explicitly, we have the following labelling scheme: for \widehat{V}_2 , labels $l_{a_1=9} = l_{a_2=11} = 1$, are the only non-zero indices; for \widehat{V}_3 the non-zero indices are $l_{a_1=5} = l_{a_2=7} = l_{a_3=9} = l_{a_4=11} = 1$; and finally for \widehat{V}_4 the non-zero indices are $l_{a_1=1} = l_{a_2=3} = l_{a_3=5} = l_{a_4=7} = l_{a_5=9} = l_{a_6=11} = 1$.

Operators V 's (omitting the unit matrix) are then cast in the form

$$\begin{aligned} \widehat{V}_2 &= \sum_{l \in \Lambda} (-1)^{l_9+l_{11}} |l_9 l_{11}\rangle \langle l_9 l_{11}|, \\ \widehat{V}_3 &= \sum_{l \in \Lambda} (-1)^{l_5+l_7+l_9+l_{11}} |l_5 l_7 l_9 l_{11}\rangle \langle l_5 l_7 l_9 l_{11}|, \\ \widehat{V}_4 &= \sum_{l \in \Lambda} (-1)^{l_1+l_3+l_5+l_7+l_9+l_{11}} |l_1 l_3 l_5 l_7 l_9 l_{11}\rangle \langle l_1 l_3 l_5 l_7 l_9 l_{11}|. \end{aligned} \quad (A12)$$

We can compare the matrix form in a computational basis of V 's in Equation (A12) to the respective ones for CZ's gates in Equation (A7), and seek to establish a relation between them. This will allow the operation algorithms formulated in terms of volume operators, to be expressed via CZ gate actions.

An application of the formulas in Equations (A10) and (A11) is to provide the inter-relation of volume operators $\{\widehat{V}_a = Z^{l_a}; a \in [4], l_a = \{l_{a_m}\}_{m=1}^n\}$ to CZ gates. Referring to Equation (A12), we have

$$\widehat{V}_a = \sum_{k+l \in \Lambda} C_{k+l,a}^\dagger U_{k+l}^{cz}. \quad (A13)$$

To finalize the proof, we introduce the *dual map*: Given an endomorphic map \mathcal{E} mapping states (observables) to themselves, consider the expectation value of an observable e.g., X , on a state $\mathcal{E}(\rho)$, viz. $\langle X, \mathcal{E}(\rho) \rangle = \text{Tr}(X \mathcal{E}(\rho))$, where map \mathcal{E} has Kraus generators representation $\mathcal{E}(\rho) = \sum_i A_i \rho A_i^\dagger$. By virtue of the cyclic property of trace, we define the dual map $\mathcal{E}^*(X) = \sum_i A_i^\dagger X A_i$, via the equation $\langle X, \mathcal{E}(\rho) \rangle = \text{Tr}(\rho \mathcal{E}^*(X))$. \square

Appendix B. Uncertainties and More

Uncertainties: Since the volume function is identified with the mean value of the quantum measurement of e.g., in the context of the second algorithm that utilized state ρ_2 and the observable M_2 , (for notational simplicity $\rho_2 \equiv \rho$, $M_2 \equiv M$, $\langle M \rangle_2 \equiv \langle M \rangle$), there will be some intrinsic quantum uncertainty in its values which can be evaluated as $\Delta M^2 \equiv \langle M^2 \rangle - \langle M \rangle^2$, by means of the observable $M^2 = 4 \sum_{a=1}^4 \lambda_a^2 P_a \otimes \mathbb{I}^{\otimes 12}$. Elaborating on the expression of the statistical moments involved in the

uncertainty, we cast ΔM^2 into the form of the expectation value of the non-positive definite extended observable $M^2 \otimes \mathbb{I}_{2^{14}} - M \otimes M$, in the state $\rho \otimes \rho$, i.e.,

$$\Delta M^2 = \text{Tr}((M^2 \otimes \mathbb{I} - M \otimes M)(\rho \otimes \rho)).$$

This result suggests that the quantum uncertainty of the volumetric measurement can be simulated by the mean value of the observable $M^2 \otimes \mathbb{I} - M \otimes M$. Computing the ratio of uncertainties of the volume operators, we find $\Delta M_{HS}^{(X)} / \Delta M_{HS,sep}^{(X)} = \frac{2}{5}, r \in [0, 1)$, which implies a large uncertainty in the measurement since both the ratios of mean-values and that of the uncertainties are equal to each other, independently of the measuring state ρ .

More general separable systems: In further recent developments on the statistics of X states, by employing matrix measures such as the Hilbert–Schmidt (HS) and Bures (B) measures, various bipartite systems of 2×2 and $2 \times K$ dimensionality have been investigated as to their separability statistics. Specifically, the kinds of manifold of parameters characterizing such bipartite systems are e.g.,: the full real $15D$ qubit-qubit manifold and the $9D$ real qubit-qubit manifold. The density matrices of the marginal systems A, B , described by their corresponding Bloch vector lengths (ball radii) r_A, r_B and the respective volumes have been investigated analytically and numerically to find values for the a priori marginal “separability probability” $p_\beta^{(\alpha)}(r) = \frac{V_{sep}^{(\alpha)}(r)}{V^{(\beta)}(r)}$, for the cases $\alpha = 2 \times K$; Re(qubits), and for $\beta = HS, B$, where $r = r_A$ or r_B . Remarkably, some constant values for the a priori probabilities are conjectured and in some cases are also numerically corroborated.

In particular, recent works by Slater [3,33] extend the investigations to the case of joint probability distribution $p_\beta^{(\alpha)}(r_A, r_B)$, based on the knowledge of marginal distributions $p_\beta^{(\alpha)}(r_A), p_\beta^{(\alpha)}(r_B)$. The work is mainly carried out numerically—except in the case of X states where analytic results can be provided. Among the findings, a new phenomenon has been spotted, named “Bloch radii repulsion”, which suggests an interesting property of the joint distribution, and it seems to be a necessary step for future progress towards analytic proofs regarding the entanglement statistics of Bloch radii of marginal subsystems. Given the more complicated polynomial character of the volume functions $V_{sep}^{(\alpha)}(r)$ in those more general cases, our preliminary investigation has shown that the simulating algorithm should be more complicated, involving more qubits with multi-particle interactions. It is worth searching for operational algorithms for the statistics of these more generalized bipartite systems as well, given the fact that any numerical generation and investigation of such statistical ensembles are rather difficult to achieve and it is prone to generating large numerical errors.

Appendix C. Hypergraphs and Volume Operator

This final appendix proceeds by showing that, by invoking the theory of hypergraphs, the volume operator \widehat{V} can be expressed as an observable determined by the adjacency tensors of a non-uniform 12 vertex hypergraph with qubits placed at each vertex—see Figure A1 below.

Let the non-uniform hypergraph $G(V, E)$ where $V = \{1, \dots, n\}$ is the vertex set and $E = E_1 \cup E_2 \dots \cup E_D$ the hyperedge set, which is the union of subsets of fixed degree hyperedges denoted $E_s \subset V^1 \cup V^2 \cup \dots \cup V^s$, for $s = 1, \dots, D$, where $D = |e|, e \in E_D$, is the maximal cardinality of a hyperedge [4–7]. Special cases of $G(V, E)$ are the k -graphs uniform hypergraphs whose hyperedge set $E \subset V^k$ contains only edges $e \in E$ with fixed cardinality $|e| = k > 2$. The case $k = 2$ corresponds to ordinary graphs.

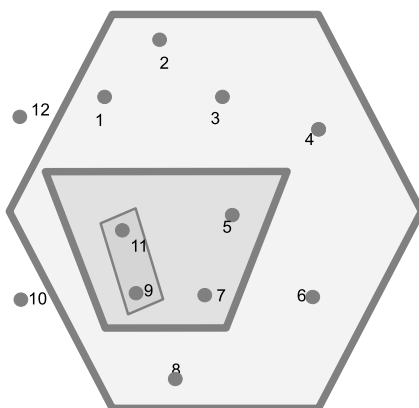


Figure A1. Non-uniform hypergraph interaction configuration of the 12-qubit lattice. Hyperedges: exagon {1,3,5,7,9,11}; trapezoid {5,7,9,11}; orthogonal {9,11}.

For our case, the hypergraph of coupled qubits is parametrized by the vertex set $V = [12] = \{1, \dots, 11, 12\}$, with $D = 6$ and hyperedges $E_2 = \{(9, 11)\}$, $E_4 = \{(5, 7, 9, 11)\}$ and $E_6 = \{(1, 3, 5, 7, 9, 11)\}$. For each uniform s -graph component hypergraph with edge set E_s , an adjacency tensor $A_s = (a_{i_1 \dots i_s}) \in \mathbb{R}^{s \times s}$ is introduced with elements

$$a_{i_1 \dots i_s} = \begin{cases} \frac{1}{(s-1)!} & \text{if } (i_1 \dots i_s) \in E_s \\ 0 & \text{if } (i_1 \dots i_s) \notin E_s. \end{cases}$$

Employing this definition to the hyperedges E_2, E_4 and E_6 , we express compactly the volume operator \hat{V} of the lattice qubit model issued in Equation (4) as

$$\begin{aligned} \hat{V} = & \mathbb{I}^{\otimes 12} - 3 \sum_{(i_1, i_2) \in E_2} a_{i_1 i_2} Z^{i_1} Z^{i_2} + 3 \sum_{(i_1, i_2, i_3, i_4) \in E_4} a_{i_1 i_2 i_3 i_4} Z^{i_1} Z^{i_2} Z^{i_3} Z^{i_4} \\ & - \sum_{(i_1, i_2, i_3, i_4, i_5, i_6) \in E_6} a_{i_1 i_2 i_3 i_4 i_5 i_6} Z^{i_1} Z^{i_2} Z^{i_3} Z^{i_4} Z^{i_5} Z^{i_6}. \end{aligned} \tag{A14}$$

References

1. Życzkowski, K.; Horodecki, P.; Sanpera, A.; Lewenstein, M. Volume of the set of separable states. *Phys. Rev. A* **1998**, *58*, 883. [\[CrossRef\]](#)
2. Milz, S.; Strunz, W.T. Volumes of conditioned bipartite state spaces. *J. Phys. A Math. Theor.* **2015**, *48*, 035306. [\[CrossRef\]](#)
3. Slater, P.B. Bloch radii repulsion in separable two-qubit systems. *arXiv* **2015**, arXiv:1506.08739.
4. Berge, C. *Hypergraphs: Combinatorics of Finite Sets*; North-Holland Mathematical Library: Amsterdam, The Netherlands, 1973; Volume 45.
5. Bretto, A. *Hypergraph Theory, an Introduction*; Springer: Berlin, Germany, 2013.
6. Qi, L.; Luo, Z. *Tensor Analysis*; SIAM: Philadelphia, PA, USA, 2017.
7. Ouvrard, X.; Le Goff, J.-M.; Marchand-Maillet, S. Adjacency and Tensor Representation in General Hypergraphs Part 1: e-adjacency Tensor Uniformisation Using Homogeneous Polynomials. *arXiv* **2017**, arXiv:1712.08189.
8. Hein, M.; Dür, W.; Eisert, J.; Raussendorf, R.; Van den Nest, M.; Briegel, H.-J. *Quantum Computers, Algorithm and Chaos*; Proceedings of the International School of Physics “Enrico Fermi”; IOS: Varena, Italy, 2005.
9. Qu, R.; Wang, J.; Li, Z.; Bao, Y. Encoding hypergraphs into quantum states. *Phys. Rev. A* **2013**, *87*, 022311. [\[CrossRef\]](#)
10. Rossi, M.; Huber, M.; Bruss, D.; Machiavello, C. Quantum hypergraph states. *New J. Phys.* **2013**, *15*, 113022. [\[CrossRef\]](#)
11. Yoshida, B. Topological phases with generalized global symmetries. *Phys. Rev. B* **2016**, *93*, 155131. [\[CrossRef\]](#)

12. Miller, J.; Miyake, A. Hierarchy of universal entanglement in 2D measurement-based quantum computation. *J. Quant. Inform.* **2016**, *2*, 16036. [[CrossRef](#)]
13. Gühne, O.; Cuquet, M.; Steinhoff, F.E.; Moroder, T.; Rossi, M.; Bruss, D.; Kraus, B.; Machiavello, C. Entanglement and nonclassical properties of hypergraph states. *J. Phys. A Math. Theor.* **2014**, *47*, 335303. [[CrossRef](#)]
14. Jozsa, R.; Linden, N. On the role of entanglement in quantum-computational speed-up. *Proc. R. Soc. A* **2003**, *8*, 2011. [[CrossRef](#)]
15. Valiant, L.G. Quantum Circuits That Can Be Simulated Classically in Polynomial Time. *SIAM J. Comput.* **2002**, *3*, 1229. [[CrossRef](#)]
16. Jozsa, R.; Miyake, A. Matchgates and classical simulation of quantum circuits. *Proc. R. Soc. A* **2008**, *464*, 3089. [[CrossRef](#)]
17. Bremner, M.J.; Jozsa, R.; Shepherd, D.J. Classical simulation of commuting quantum computations implies collapse of the polynomial hierarchy. *Proc. R. Soc. A* **2011**, *467*, 459. [[CrossRef](#)]
18. Ni, X.; van den Nest, M. Commuting quantum circuits: efficient classical simulations versus hardness results. *Quant. Inform. Comput.* **2013**, *13*, 54.
19. Nakata, Y.; Koashi, M.; Mura0, M. Generating a state t-design by diagonal quantum circuits. *New J. Phys.* **2014**, *16*, 053043. [[CrossRef](#)]
20. Nakata, Y.; Mura0, M. Diagonal quantum circuits: Their computational power and applications. *Eur. Phys. J. Plus* **2014**, *129*, 152. [[CrossRef](#)]
21. Fujii, K.; Morimae, T. Commuting quantum circuits and complexity of Ising partition functions. *New J. Phys.* **2017**, *19*, 033003. [[CrossRef](#)]
22. Lechner, W.; Hauke, P.; Zoller, P. A quantum annealing architecture with all-to-all connectivity from local interactions. *Sci. Adv.* **2015**, *1*, e1500838. [[CrossRef](#)]
23. Glaetzle, A.; van Bijnen, R. M. W.; Zoller, P.; Lechner, W. A coherent quantum annealer with Rydberg atoms. *Nat. Comm.* **2017**, *8*, 15813. [[CrossRef](#)] [[PubMed](#)]
24. Sargent, M., III; Scully, M.O.; Lamb, W.E., Jr. *Laser Physics*; Westview Press: Boulder, CO, USA, 1978.
25. Bush, P.; Lahti, P.J.; Mittelstaedt, P. *The Quantum Theory of Measurement*; Springer: Berlin, Germany, 1991.
26. Englert, B.G.; Wodkiewicz, K. Intrinsic and operational observables in quantum mechanics. *Phys. Rev. A* **1995**, *51*, 2661. [[CrossRef](#)]
27. Ellinas, D.; Tsochantjis, I. Region operators of Wigner function: Transformations, realizations and bounds. *Rep. Math. Phys.* **2006**, *57*, 69. [[CrossRef](#)]
28. Ellinas, D.; Bracken, A.J. Phase-space-region operators and the Wigner function: Geometric constructions and tomography. *Phys. Rev. A* **2008**, *78*, 052106. [[CrossRef](#)]
29. Yu, T.; Eberly, J.H. Evolution from entanglement to decoherence of bipartite mixed "X" states. *Quant. Inf. Comp.* **2007**, *7*, 459.
30. Ali, M.; Alber, G.; Rau, A.R.P. Manipulating entanglement sudden death of two-qubit X-states in zero- and finite-temperature reservoirs. *J. Phys. B* **2009**, *42*, 025501. [[CrossRef](#)]
31. Rau, A.R.P. Algebraic characterization of X-states in quantum information. *J. Phys. A* **2009**, *42*, 412002. [[CrossRef](#)]
32. Steeb, W.-H.; Hardy, Y. Exponential of a matrix, a nonlinear problem, and quantum gates. *J. Math. Phys.* **2015**, *56*, 012201. [[CrossRef](#)]
33. Slater, P.B. Two-Qubit Separability Probabilities as Joint Functions of the Bloch Radii of the Qubit Subsystems. *Inter. J. Quant. Info.* **2016**, *14*, 1650042. [[CrossRef](#)]

